0.4) × 10^{-11} for ^{85}Kr and (1.0 ± 0.4) × 10^{-12} for ^{81}Kr, which are in good agreement with previous measurements using other methods (*3, 8, 13*). The capture efficiencies can be calibrated with enriched samples of known isotopic abundance to correct for any isotope-dependent effects and to measure isotopic ratios in unknown samples.

Our system has achieved an efficiency of 10^{-7}. Use of this system to measure the abundance of ^{85}Kr to within 10% would require 2 hours and a krypton sample of 3 ml, whereas measurement of ^{81}Kr to within 10% would require 2 days and a sample of 60 ml. This limits the current system to atmospheric applications in which large samples of gas are readily available. It is possible to raise the efficiency many orders of magnitude through improvements such as cryogenic cooling in the discharge region (*24*) and recirculation of krypton gas (*25*). Other proposed schemes (*26*) with an ultraviolet (UV) laser instead of a dc discharge to excite the atoms to the metastable level via a two-photon transition could dramatically improve detection efficiency.

ATTA can be applied to many different isotopes (Table 1). Laser trapping is well established on alkali, alkali earth, and noble gas elements. Trapping other elements is generally more difficult because of both the complexity of their ground-level structures and the lack of suitable UV lasers. Some of these problems may be overcome with future advances in UV laser technology.

References and Notes

1. J. R. Arnold and W. F. Libby, *Science* **113**, 111 (1951).
2. R. A. Muller, *Science* **196**, 489 (1977); D. E. Nelson *et al.*, *Science* **198**, 507 (1977); C. L. Bennett *et al.*, *Science* **198**, 508 (1977).
3. International Atomic Energy Agency, *Isotope of Noble Gases as Tracers in Environmental Studies* (International Atomic Energy Agency, Vienna, Austria, 1992).
4. *Proc. Sixth International Conference on AMS, Nucl. Instr. Meth.* **123** (1997).
5. S. Baumgartner *et al.*, *Science* **279**, 1330 (1998).
6. R. Davis Jr., A. K. Mann, L. Wolfenstein, *Annu. Rev. Nucl. Part. Sci.* **39**, 467 (1989); J. N. Bahcall and R. K. Ulrich, *Rev. Mod. Phys.* **60**, 297 (1988).
7. R. A. Muller, L. W. Alvarez, W. R. Holley, E. J. Stephenson, *Science* **196**, 521 (1977); R. N. Cahn and S. L. Glashow, *Science* **213**, 607 (1981).
8. H. H. Loosli and H. Oeschger, *Earth Planet. Sci. Lett.* **7**, 67 (1969).
9. F. von Hippel, D. H. Albright, B. G. Levi, *Sci. Am.* **253**, 40 (Sept., 1985).
10. H. Oeschger, *Nucl. Instrum. Methods Phys. Res. B* **29**, 196 (1987).
11. J. R. Petit *et al.*, *Nature* **399**, 429 (1999); C. Lorius *et al.*, *Nature* **316**, 591 (1985).
12. G. S. Hurst, M. G. Payne, S. D. Kramer, C. H. Chen, *Phys. Today* **33**, 24 (Sept. 1980)
13. P. Collon *et al.*, *Nucl. Instr. Meth.* **B123**, 122 (1997); P. Collon, thesis (University of Vienna, Austria, 1999).
14. V. S. Letokhov, *Laser Photoionization Spectroscopy* (Academic Press, Orlando, 1987); G. S. Hurst and M. G. Payne, *Principles and Applications of Resonance Ionisation Spectroscopy* (Adam Hilger, Bristol, UK, 1988).
15. R. D. LaBelle, C. S. Hansen, M. M. Mankowski, W. M. Fairbank Jr., *Phys. Rev. A* **54**, 4461 (1996); B. D. Cannon and T. J. Whitaker, *Appl. Phys. B* **38**, 57 (1985).
16. S. D. Kramer *et al.*, *Nucl. Instrum. Methods Phys. Res. B* **17**, 395 (1986).
17. M. Walhout, H. J. L. Megens, A. Witte, S. L. Rolston, *Phys. Rev. A* **48**, R879 (1993); F. Shimizu, K. Shimizu, H. Takuma, *Chem. Phys.* **145**, 327 (1990).
18. W. Phillips and H. Metcalf, *Phys. Rev. Lett.* **48**, 596 (1982); T. E. Thomas, S. W. Dapore-Schwartz, M. D. Ray, G. P. Lafayatis, *Phys. Rev. Lett.* **67**, 3483 (1991).
19. E. L. Raab, M. Prentiss, A. E. Cable, S. Chu, D. E. Pritchard, *Phys. Rev. Lett.* **59**, 2631 (1987).
20. Z. Hu and H. J. Kimble, *Opt. Lett.* **19**, 1888 (1994); D. Haubrich *et al.*, *Europhys. Lett.* **34**, 663 (1996).
21. B. D. Cannon, *Phys. Rev. A* **47**, 1148 (1993).
22. Metastable atoms quench upon colliding with walls; therefore, they do not exist in background as a vapor. In other applications when ground-level atoms are used, cryopanels can be installed to reduce the density of background atoms.
23. Rate calculations are based on loading time only, which is one-half of real time.
24. W. Roojakkers, W. Hogervorst, W. Vassen, *Opt. Commun. B* **123**, 321, (1996).
25. B. E. Lehman, D. F. Rauber, N. Thonnard, R. D. Willis, *Nucl. Instrum. Methods Phys. Res. B* **28**, 571 (1987).
26. G. S. Hurst, M. G. Payne, R. C. Phillips, J. W. T. Dabbs, B. E. Lehmann, *J. Appl. Phys.* **55**, 1278 (1984).
27. W. Henning *et al.*, *Science* **236**, 725 (1987).
28. K. Zimmer *et al.*, *Appl. Phys. B* **59**, 117 (1994).
29. J.-H. Chao and C.-L. Tseng, *Nucl. Instrum. Methods Phys. Res. A* **372**, 275 (1996).

30. Supported by the U.S. Department of Energy, Nuclear Physics Division. L.Y. was supported by the Office of Basic Energy Sciences, Division of Chemical Sciences (contract W-31-109-ENG-38). We thank C. Wieman and W. Kutschera for stimulating discussions. In particular, Z.-T.L. had private communications with C. Wieman about Wieman's earlier proposal to count ^{90}Sr atoms with a MOT. We also thank D. Lin for his contribution to the earlier phase of this project, M. Walhout for showing us discharge designs, and B. Cannon for calculating the hyperfine structure of ^{81}Kr.

12 July 1999; accepted 27 September

Similarity of the *C. elegans* Developmental Timing Protein LIN-42 to Circadian Rhythm Proteins

Mili Jeon,[1]* Heather F. Gardner,[2]* Eric A. Miller,[2]† Jodie Deshler,[2]‡ Ann E. Rougvie[1,2]§

The *Caenorhabditis elegans* heterochronic genes control the relative timing and sequence of many events during postembryonic development, including the terminal differentiation of the lateral hypodermis, which occurs during the final (fourth) molt. Inactivation of the heterochronic gene *lin-42* causes hypodermal terminal differentiation to occur precociously, during the third molt. LIN-42 most closely resembles the Period family of proteins from *Drosophila* and other organisms, proteins that function in another type of biological timing mechanism: the timing of circadian rhythms. *Per* mRNA levels oscillate with an approximately 24-hour periodicity. *lin-42* mRNA levels also oscillate, but with a faster rhythm; the oscillation occurs relative to the approximately 6-hour molting cycles of postembryonic development.

The timing of distinct biological processes within a cell or organism is carefully controlled. One class of temporal regulators, exemplified by the *C. elegans* heterochronic genes, times the onset of developmental events. These genes control the relative timing of diverse stage-specific events during postembryonic development such as dauer larva formation, vulva formation, and the terminal differentiation of the hypodermis (*1*). In other organisms, members of this general heterochronic gene class include the *Teopod* genes and *Glossy15* of maize, *hasty* of *Arabidopsis*, and *anachronism* of *Drosophila* (*2*). Mutations in these genes either advance or retard expression of certain developmental programs.

A second class of temporal regulators comprises the "clock" components that regulate circadian rhythms, the approximately 24-hour periodicity of biological processes such as sleep-wake cycles in humans (*3*). Genes that control circadian rhythms have been cloned from several organisms, including *Drosophila*, *Neurospora*, and mouse. Although shared motifs have been observed between certain circadian rhythm proteins, shared motifs between these proteins and the timing factors that control developmental progression have not been reported previously. Here we demonstrate that the *C. elegans* heterochronic gene *lin-42* encodes a protein

[1]Department of Biochemistry, Molecular Biology, and Biophysics; [2]Department of Genetics, Cell Biology, and Development, University of Minnesota, St. Paul, MN 55108, USA.

*These authors contributed equally to this work.
†Present address: Department of Epidemiology, University of North Carolina, Chapel Hill, NC 27599, USA.
‡Present address: Department of Biology, University of Wisconsin, River Falls, WI 54022, USA.
§To whom correspondence should be addressed.

with similarity to the *Drosophila period* protein (PER) and its counterparts in other organisms. This discovery provides a molecular connection between these two types of cellular timekeepers.

Caenorhabditis elegans proceeds through four postembryonic larval stages (L1 to L4) on the way to adulthood. During the fourth (final) molt, the lateral hypodermal seam cells terminally differentiate; they exit the cell cycle and secrete a morphologically distinct adult cuticle. Mutations in the heterochronic genes alter the timing of this event. Loss-of-function mutations in the heterochronic genes *lin-14*, *lin-28*, and *lin-42* cause precocious phenotypes in which seam cell terminal differentiation is executed prematurely, whereas mutation of *lin-4* or *lin-29* retards this differentiation event (*1, 4*). These latter mutants undergo additional rounds of ecdysis during which the hypodermis remains undifferentiated. These genes form a negative regulatory pathway that restricts seam cell terminal differentiation to the fourth molt (*5*). The transcription factor LIN-29 is the most direct trigger of the switch to the adult hypodermal program; the remaining genes act upstream, ensuring that *lin-29* activity is correctly timed. We cloned and characterized *lin-42* to better understand its role in this developmental timing mechanism.

Genetic mapping using a combination of visible markers and restriction fragment length polymorphism (RFLP) markers placed *lin-42* on the left arm of linkage group II (LGII) between *veP2* and *nP48*, nearer to *veP2* (Fig. 1A) (*6*). Because of the paucity of genetic or molecular markers in this region, we chose a transposon tagging approach to identify the *lin-42* locus within the interval from *veP2* to *nP48* (*veP2-nP48*). We searched for *lin-42* alleles induced by insertion of the Tc1 transposon (*7*). *lin-42* alleles can be isolated efficiently among mutations that restore adult cuticle synthesis in a *lin-4* mutant background (*8*), where seam cell terminal differentiation would otherwise not occur. We identified 34 mutations that restore adult cuticle to *lin-4* mutants, presumably as a result of Tc1-mediated gene disruptions. To identify candidate *lin-42* mutations among these, we performed a secondary screen for animals resembling previously analyzed *lin-42 lin-4* double mutants. For example, *lin-42* mutations do not suppress the vulvaless phenotype of *lin-4* mutants or their inability to form dauer larvae (*8*). Mutants meeting these criteria were outcrossed to separate the new mutation from *lin-4*. Two of the outcrossed mutants contain new *lin-42* alleles based on the following properties of the new mutations: (i) they cause precocious adult cuticle synthesis during the third molt, (ii) they show weak linkage to *lin-4* [*lin-42* and *lin-4* are approximately 12 centimorgans (cM) apart on LG II], and (iii) they fail to complement an existing *lin-42* allele, *ve16*. We sequenced genomic DNA flanking the Tc1 element responsible for the *lin-42* lesion in the *ve27* allele and used it to search the *C. elegans* genome sequence. In agreement with the genetic map location of *lin-42*, the sequence identified cosmid F47F6, which maps to the *veP2-nP48* interval on LG II, nearer to *veP2* (Fig. 1A).

Transformation with cosmid F20E9, which extensively overlaps F47F6 (Fig. 1A) (*9*), rescued the precocious phenotype of *lin-42* mutants. The *lin-42*–rescuing activity was further delimited by the injection of F20E9 subclones and a polymerase chain reaction (PCR) fragment from the region. The smallest rescuing fragment was an 8.9-kb Sac II fragment that spanned the *ve27* Tc1 insertion site and contained a single large open reading frame based

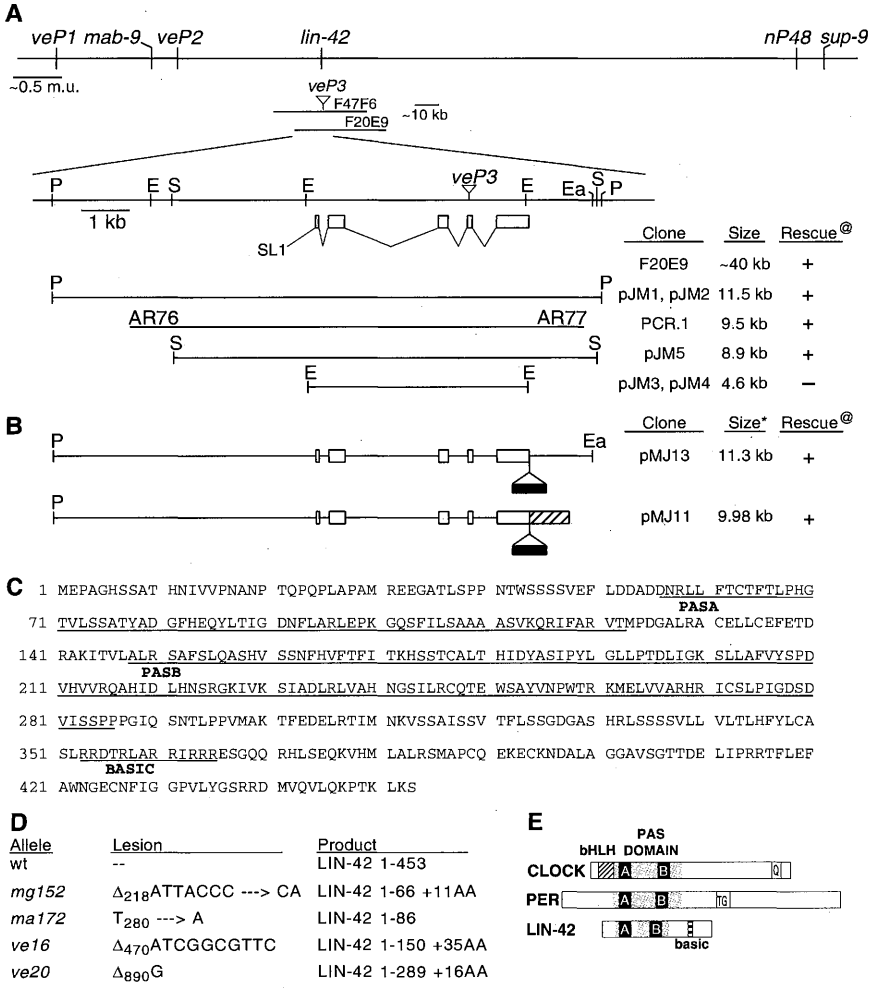

Fig. 1. Analysis of the *lin-42* locus and alleles. (**A**) The top line represents the genetic map of the left arm of LGII. The placement of *mab-9* between *veP1* and *veP2* is predicted from map distances. Cosmids identified by sequences flanking the *lin-42* allele-specific Tc1, *veP3*, are indicated below the genetic map. The region corresponding to the *lin-42* locus is expanded and shown relative to restriction sites Pst I (P), Eco RI (E), Eag I (Ea), and Sac II (S). Beneath the DNA line is the predicted structure of the *lin-42* coding region. Exons are shown by open boxes. *lin-42* is trans-spliced to SL1 20 nt 5′ to the translation initiation codon. @, summary of the transformation rescue experiments: + indicates that >90% of the L3 molt seam cells were wild type and thus lacked adult alae; – indicates that >90% of the seam cells were mutant and synthesized adult alae precociously. (**B**) Diagrams of *lin-42::gfp* fusions and a summary of their rescuing ability. The *gfp* open reading frame is indicated by the solid rectangle. *unc-54* 3′ UTR is indicated by the hatched rectangle. *, the size given for these constructs does not include *gfp* or *unc-54* sequences. (**C**) The predicted amino acid sequence of the longest *lin-42* open reading frame (*35*). (**D**) The effect of *lin-42* lesions on the predicted *lin-42* protein product. The locations of the lesions are indicated with respect to the first nucleotide of the cDNA (after the trans-spliced leader), which occurs 20 nt 5′ to the ATG. Triangles indicate a deletion of the subsequent base pairs. Arrows indicate a replacement with the indicated base pairs. AA, amino acid. (**E**) Domain organizations of CLOCK, PER, and LIN-42. The direct repeats of the PAS domain are indicated by black boxes labeled A and B. The gray areas flanking the direct repeats indicate the extents of the PAS domains. CLOCK contains a bHLH domain in its NH_2-terminus (hatch marks) and a glutamine repeat (Q) in its COOH-terminus (*36*), and PER contains a glycine-threonine repeat in its COOH-terminus (TG). LIN-42 contains a basic region COOH-terminal to its PAS domain (dark shading).

on GeneFinder predictions (*9*) (Fig. 1A). The Tc1 element was inserted into the fourth of five predicted exons, and it eliminated the COOH-terminal half of the 453–amino acid predicted protein.

To confirm that this gene corresponds to *lin-42*, we determined the DNA sequence of the predicted exons from four other *lin-42* alleles. Each of these mutations results in a COOH-terminal truncation of the predicted *lin-42* protein product (Fig. 1D). *mg152* produces the most severe truncation, yielding a protein containing only the NH_2-terminal 66 amino acids, and is likely to be a null mutation.

We confirmed the *lin-42* gene structure by reverse transcription–PCR (RT-PCR) (*10*). Sequence analysis of RT-PCR products spanning overlapping portions of the five exons revealed that the GeneFinder prediction is accurate (Fig. 1).

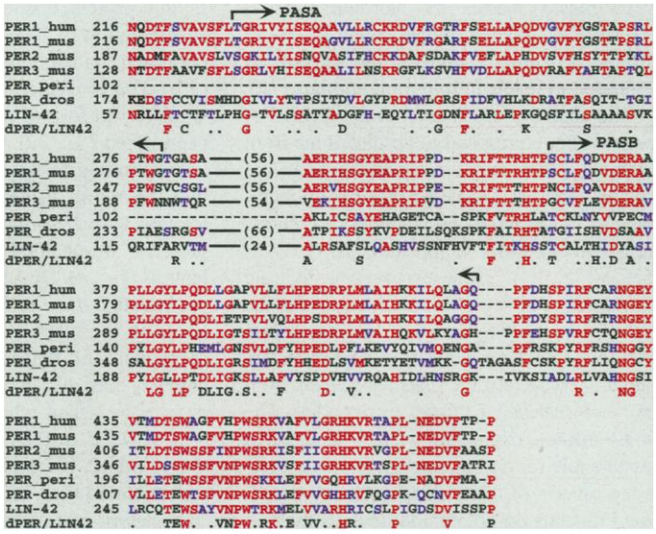

Fig. 2. Sequence alignments comparing LIN-42 to the PER-related proteins from mammals, *Drosophila*, and cockroach. Amino acids identical in at least 50% of the proteins are indicated in red, and similarities are indicated in blue (*35*). The dPER/LIN42 line indicates conservation with emphasis on LIN-42 and dPER. Red letters indicate amino acids that are conserved among all six proteins. Black letters indicate identities, and single dots indicate similarities between LIN-42 and dPER. The PASA and PASB repeats (*12*) are indicated (arrows). *Periplanta americana* sequence is unavailable for the PASA region. When the GT repeat of *Drosophila* PER is omitted from BLAST or tFASTA searches, LIN-42 is the closest match to PER in the *C. elegans* genome. GenBank accession numbers are as follows: human PER1_hum, AF022991; mouse PER1_mus, AF022991; mouse PER2_mus, AF035830; mouse PER3_mus, AF050182; *Drosophila* PER_dros, P07663; American cockroach *Periplanta americana* PER_peri, U12772; and LIN-42, AF183400.

Database searches reveal that the *lin-42* protein is most similar to members of the PERIOD (PER) family of circadian rhythm proteins from insects and mammals. The most striking region of similarity includes a protein interaction domain, the PAS domain (*11*), which has recently come to be viewed as a signature feature of circadian rhythm proteins, including the insect and mammalian PER proteins, the WHITE COLLAR proteins of *Neurospora*, and the CLOCK and BMAL proteins of mice and their *Drosophila* counterparts, dCLOCK and CYC (*3*). The PER PAS domain is an approximately 260–amino acid region containing two divergent hydrophobic direct repeats of about 50 amino acids, known as the PASA and PASB repeats (Fig. 2) (*11, 12*). The region of highest similarity between LIN-42 and PER encompasses the PASB repeat (Fig. 2) and includes the cytoplasmic localization domain (CLD) of PER (*13*). The two proteins are 30% identical and 45% similar throughout this 139–amino acid region. The percent identity between LIN-42 and other PER family members in this region is also about 30% (29% for cockroach PER; 28% for human and mouse PER1). By comparison, human PER1 (hPER1) and *Drosophila* PER share 39% identity in this region. The similarity between vertebrate and invertebrate PER proteins is lower in the PASA repeat. *Drosophila* PER and LIN-42 each share 20% identity with hPER1 over the 50–amino acid PASA repeat (Fig. 2).

The PAS domain was originally named for its presence in PER, the aryl hydrocarbon receptor nuclear translocator (ARNT), and the *Drosophila single-minded* protein (SIM) (*11*).

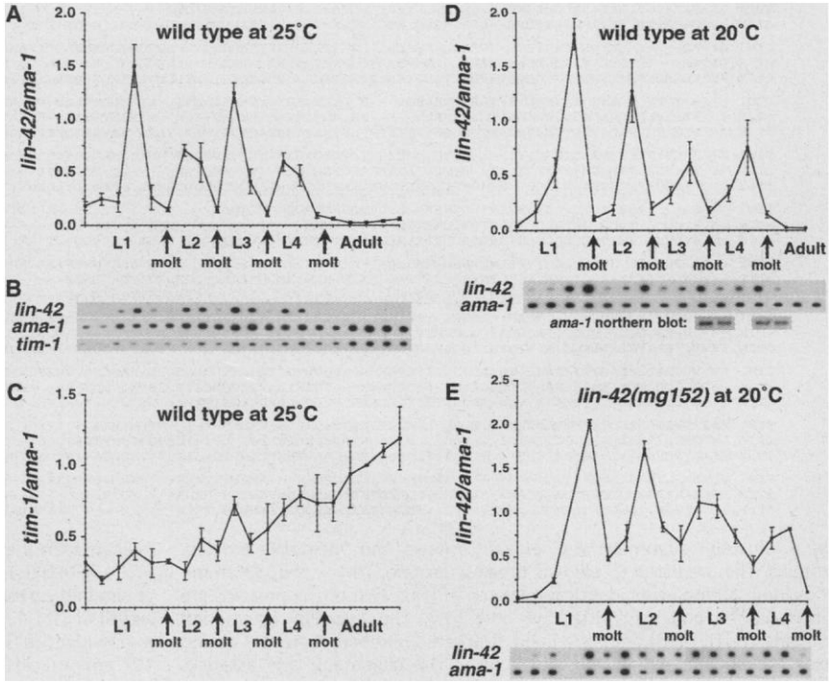

Fig. 3. *lin-42* and *tim-1* mRNA levels during postembryonic development. (**A**) Graph showing the relative abundance over time of the *lin-42* transcripts, expressed as a ratio of the amount of their amplified products to that of the *ama-1* transcript for each RT-PCR reaction (*17*). The tick marks on the *x* axis indicate 2-hour intervals of postembryonic development at 25°C after L1 larval arrest. Error bars are ±1 SE. Variances were computed empirically with the use of a large sample approximation. (**B**) Autoradiograms of RT-PCR products from *lin-42*, *ama-1*, and *tim-1* amplifications analyzed by Southern blotting. Data are representative of experiments graphed in (A) and (C). (**C**) Graph of *tim-1* mRNA levels relative to *ama-1* levels for each RT-PCR reaction. Details are as in (A). The signals for *lin-42* and *tim-1* depend on specific activities of the probes used and exact washing conditions (*16*) and therefore cannot be directly compared. (**D**) Top panel, graph of an experiment as in (A), except that the animals were reared at 20°C and the tick marks on the *x* axis indicate 3-hour intervals of postembryonic development. Bottom panel, representative autoradiograms of the data graphed and the results of a Northern blot of 10 μg of total RNA probed with *ama-1* sequences. The Northern blot lanes are shown beneath the samples to which they correspond. (**E**) Results of an experiment as in (D), except that *lin-42(mg152)* animals were used. *lin-42(mg152)* development is delayed relative to that of the wild type.

Basic helix-loop-helix (bHLH) motifs are found NH_2-terminal to the PAS domain in several PAS proteins, including ARNT, SIM, CLOCK, and BMAL (*3*). *Drosophila* PER and LIN-42 both lack bHLH domains in their NH_2-termini. However, a basic region COOH-terminal to the LIN-42 PAS domain (Fig. 1C) is followed by stretches of predicted alpha helix based on PHDsec (*14*). Among all of the circadian and noncircadian PAS domain–containing proteins identified to date, the LIN-42 PAS domain most closely resembles that of the PER family. Similarly, BLAST and tFASTA algorithms identify LIN-42 as the closest match to *Drosophila* PER in the essentially complete *C. elegans* sequence database (Fig. 2).

In addition to encoding a PAS domain protein, another hallmark of *per* is that its mRNA levels oscillate with a 24-hour periodicity (*15*). To test whether mRNA oscillation is also a feature of *lin-42* expression, we examined the accumulation of *lin-42* mRNA during development at 25°C and found that *lin-42* mRNA levels cycle during each larval stage (Fig. 3, A and B). We performed RT-PCR on cDNA pools derived from synchronized worm populations sampled at 2-hour intervals during postembryonic development (*16, 17*). In these experiments, the quantity of *lin-42* cDNA amplification product was measured relative to that of *ama-1* amplified from the same pools as a control for the amount of mRNA originally present in the sample. *ama-1* encodes the large subunit of RNA polymerase II, and its mRNA abundance is essentially constant throughout postembryonic development (*16, 18*) (Fig. 3D).

The *lin-42* and *ama-1* signals were quantified (*17*), and the relative levels of *lin-42: ama-1* mRNA are graphed in Fig. 3A with respect to developmental time. Relative to *ama-1*, *lin-42* mRNA levels peak during the intermolt periods, approximately 3 hours before each molt, and decline dramatically during ecdysis. After the L4-to-adult molt, *lin-42* mRNA levels remain low. Examination of synchronized worms by Northern (RNA) analysis also reveals lower levels of *lin-42* mRNA in animals undergoing ecdysis as compared to levels in intermolt animals (*19*).

The observed oscillations of *lin-42* mRNA levels do not correspond to absolute time from hatching; rather, they are synchronized to the molting cycles as is demonstrated by the lengthening of the period of oscillation when worms are grown at a lower temperature (20°C versus 25°C) (Fig. 3D). These experiments indicate that *lin-42* mRNA levels oscillate relative to the execution of molting cycles. *C. elegans* undergoes four rounds of ecdysis, at approximately 6-hour intervals (at 25°C), as they develop from the newly hatched L1 larva to the adult. The *lin-42* mRNA expression pattern suggests a possible role for *lin-42* in promoting or coordinating aspects of the molting cycle. However, *lin-42* mutants do not exhibit obvious molting defects until the execution of the final molt (*8*). At this stage, *lin-42* mutants often have difficulty shedding the L4 cuticle. This observation suggests that *lin-42* functions in at least this ecdysis event, and perhaps another factor supplies this function during the earlier molts. During each molt cycle, a new worm cuticle is synthesized, composed mainly of collagens. Expression levels of six collagen genes have been found to oscillate relative to the molting cycles (*16*), raising the possibility that *lin-42* cycling could function in, or be synchronized with, collagen gene regulation.

In *Drosophila*, PER is regulated in part through interaction with a second circadian rhythm protein, encoded by *timeless* (*3*). The accumulation of *timeless* mRNA cycles with periodicity indistinguishable from that of *per* (*20*). The existence of a worm gene with similarity to fly and mammalian *timeless* has been noted (*21, 22*). We sequenced cDNAs corresponding to this gene, *tim-1*, and found that the worm protein shares 23 and 37% identity with *Drosophila* and mouse *timeless* proteins, respectively, across their entire lengths (Fig. 4). BLAST and tFASTA searches show that *tim-1* is the best match to TIMELESS in the worm genome. Thus, a second component of the fly circadian regulation pathway has also been conserved in *C. elegans*. We asked whether the temporal pattern of *tim-1* mRNA accumulation parallels that of *lin-42*. Unlike coordinated *per* and *tim* expression in flies, the worm *timeless* expression pattern was distinguishable from that of *lin-42* in the RT-PCR assay, and it did not oscillate with each molt (Fig. 3, B and C). In general, *tim-1* mRNA levels increase during late postembryonic development and, unlike

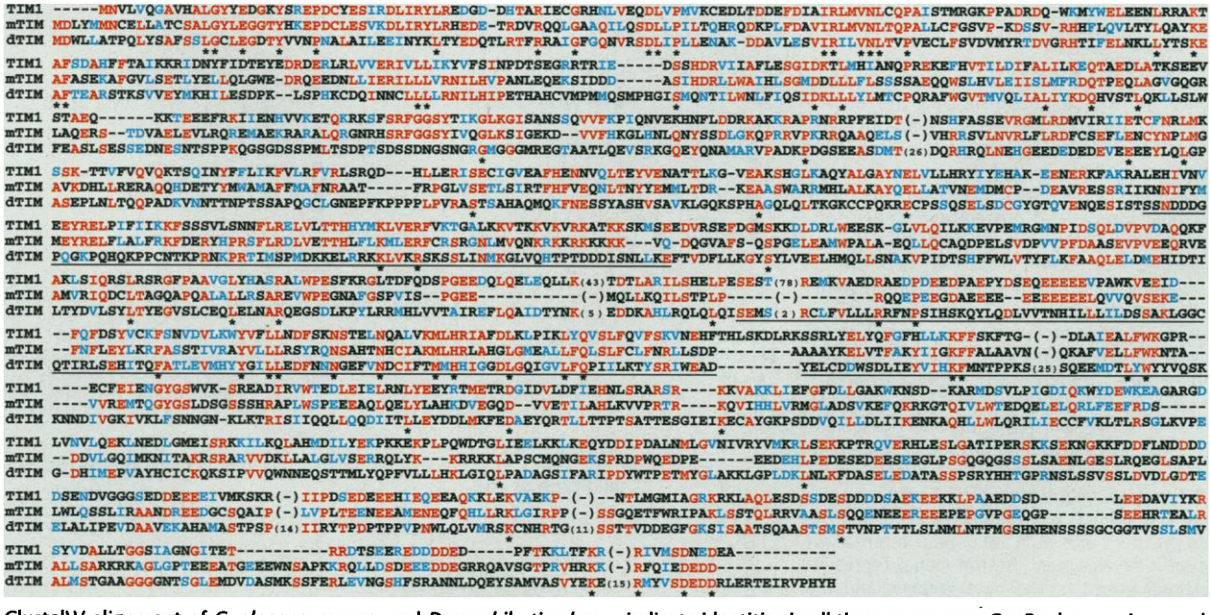

Fig. 4. ClustalW alignment of *C. elegans*, mouse, and *Drosophila timeless* proteins. The predicted *C. elegans timeless* protein, TIM-1, is 1353 amino acids long. Amino acids identical between at least two of the proteins are shown in red and similarities are blue (*35*). The two PER interaction domains in dTIM (*13*) are underlined. Bracketed numbers represent amino acids not shown; dashes indicate gaps in the alignment; and asterisks indicate identities in all three sequences. GenBank accession numbers are mTIM AF098161, dTIM AF032410, and TIM-1 AF183401. Percent identity or similarity between these proteins was calculated relative to the total length of TIM-1. The two largest gaps in the alignment are due largely to a 47% identical direct repeat in TIM-1 of a lysine-rich region followed by 102 amino acids.

lin-42 mRNA, *tim-1* mRNA is most abundant in adults.

In flies, PER and TIM participate in a negative autoregulatory feedback loop that is largely responsible for their mRNA oscillations. This regulation is dependent on their heterodimerization through the PER PAS domain and subsequent nuclear translocation (*13, 23, 24*). Neither PER nor TIM binds DNA; rather, they are thought to repress their own transcription through interaction and interference with their positive regulators, the bHLH transcription factors dCLOCK and CYC (*25*). Loss-of-function *per* mutations result in arrhythmic flies and abolish mRNA oscillations (*15*). In contrast, the cycling of *lin-42* mRNA levels occurs in the absence of functional *lin-42* protein (Fig. 3E), which indicates the lack of an autoregulatory feedback circuit.

To investigate the expression pattern of LIN-42, we generated transgenic animals bearing *lin-42::gfp* fusion constructs (Fig. 1B) (*26*). These constructs rescue the precocious phenotype of *lin-42* mutants, which suggests that the fusion protein is functional. Consistent with the *lin-42* phenotype, LIN-42::GFP is present in the lateral hypodermis (Fig. 5). LIN-42::GFP also accumulates in the hyp7 syncytium, which comprises the main body hypodermis, and in head and tail hypodermal cells. LIN-42::GFP expression is first detected in late embryonic stage animals, and it remains detectable into the adult stage. Although we have not quantitated LIN-42::GFP signals, the intensity of *lin-42::gfp* expression appears higher, in general, in animals undergoing ecdysis. In terms of subcellular accumulation, LIN-42::GFP is generally enriched in nuclei relative to cytoplasm (Fig. 5), but there is no developmental time when LIN-42::GFP is observed to be entirely nuclear or entirely cytoplasmic. Cytoplasmic LIN-42::GFP signal is enhanced in lateral seam cells during the molt periods. During the first three molts, this correlates with seam cell divisions and may be related to cell cycle stage, reflecting nuclear release followed by protein turnover and replenishment after division, because there is a period during cytokinesis where LIN-42::GFP is not observed. However, the LIN-42::GFP signal is also enhanced in the seam cell cytoplasm of L4 molt animals, when cell divisions do not occur. More detailed analysis of LIN-42 levels and subcellular localization awaits immunodetection of the endogenous protein.

One role of LIN-42 is to restrict the hypodermal accumulation of LIN-29 to the L4 stage. In *lin-42* mutant animals, LIN-29 accumulates early, during the third larval stage (*27*), indicating that *lin-42*, like *lin-14* and *lin-28*, exerts its control of seam cell terminal differentiation by restricting LIN-29 accumulation to the proper time. LIN-42 may be a more direct regulator of LIN-29 accumulation than are LIN-14 and LIN-28 because these latter proteins disappear by the end of the L1 and L2 stages, respectively (*28, 29*). *lin-14* and *lin-28* are each directly regulated by *lin-4* through the binding of the regulatory 22-nucleotide (nt) *lin-4* RNA to complementary sequences in their 3′ untranslated regions (UTRs) (*29, 30*). In contrast, *lin-42* is not likely to be a direct target of *lin-4* RNA. Searches of genomic DNA downstream from the *lin-42* stop codon have failed to reveal *lin-4* complementary sequences such as those found in the *lin-14* and *lin-28* 3′UTRs.

It has been proposed that progressive reduction in the levels of LIN-14 and LIN-28 during the first three larval stages specifies the L1-L2-L3 stage transitions in the lateral hypodermis (*29*). Null mutations in these genes result in precocious terminal differentiation as a consequence of omitting L1 (*lin-14*) or L2 (*lin-28*) seam cell division programs, which are replaced by later stage programs. In contrast, cell lineage analysis suggests that *lin-42* null mutations do not cause seam cell lineage defects during the first two larval stages (*4, 31*), which indicates that a unique requirement for LIN-42 action may be limited to the L3 stage. Wild-type *lin-42* activity could be required to promote the L3 stage identity of seam cells or to repress the L4 stage identity until the correct time. *lin-42* mutations enhance L2-stage defects of a weak *lin-14* allele (*4*), suggesting that *lin-42* may also play an earlier, nonessential role in the specification of seam cell division patterns. Expression of the *lin-42::gfp* fusion in L1 and L2 stage animals is consistent with this result.

LIN-42 activity may be stage-specifically modified by interaction through its PAS domain with different partner proteins at different developmental times. These interactions could include homotypic binding to other PAS domain–containing proteins [as seen in ARNT interaction with the aryl hydrocarbon receptor (*32*)] or heterotypic binding to non–PAS domain–containing proteins, as exemplified by the *Drosophila* PER-TIM interaction (*23*). TIM-1 is one candidate partner; others include the products of heterochronic genes identified by mutational analysis. However, none of the heterochronic mutants described to date possess phenotypes identical to those of *lin-42* mutants, which indicates that if there are LIN-42 binding partners among the products encoded by these genes, the proteins do not require each other for all aspects of their function.

Biological rhythms such as the ultradian rhythm of defecation have been studied in the soil-living nematode *C. elegans* (*33*), but circadian rhythms have not been reported. Nevertheless, we have identified *lin-42* and *tim-1* as *C. elegans* counterparts to the *per* and *timeless* genes, respectively, of flies and vertebrates. The similarity between *lin-42* and *per* extends beyond sequence conservation to the level of gene expression, as demonstrated by their oscillating mRNA levels. These results suggest an evolutionary link between these two timing mechanisms. In addition to these similarities between *per* and *lin-42*, we have observed some interesting differences. Their functions have been adapted to control timing in different contexts: PER controls circadian time but LIN-42 controls developmental time. The periods of their message-level oscillations are also altered to reflect this difference, shortened from 24 hours for *per* to ~6 hours for *lin-42*, which correlates with the execution of molts. Finally, in contrast to PER autoregulation, LIN-42 is not required to generate its own mRNA expression pattern. Thus, some features of the circadian timing mechanism appear to have been evolutionarily conserved with LIN-42 while others have diverged. An alternative view is that PER and LIN-42 represent a remarkable example of convergent evolution involving amino acid sequence, cyclical expression pattern, and type of biological process. The challenge for the future is to provide a more comprehensive comparison of the molecular components between these systems by identifying LIN-42 binding partners and the factors responsible for *lin-42* cycling.

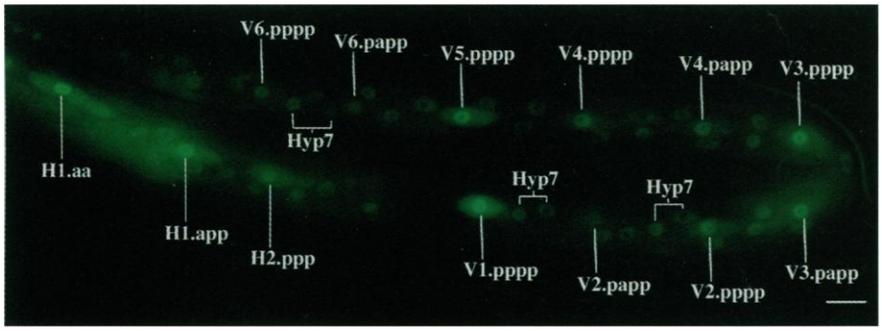

Fig. 5. Expression of *lin-42::gfp*. Fluorescence micrograph of an L3 molt stage *lin-42(mg152); vels26* animal folded back on itself so that the anterior is at the lower left. The integrated array contains pMJ11 (Fig. 1). Seam cell nuclei are labeled, as is a subset of Hyp7 nuclei. The seam cells are preparing to undergo their final division, with the exception of H1.aa, which does not divide again. High levels of GFP fluorescence are observed in nuclei of Hyp7 and the lateral seam. Cytoplasmic expression can be seen in the seam cells and is most intense in V1.pppp. Scale bar, 10 μm.

References and Notes

1. V. Ambros, in *C. elegans II*, D. L. Riddle, T. Blumenthal, B. J. Meyer, J. R. Priess, Eds. (Cold Spring Harbor Laboratory Press, Cold Spring Harbor, NY, 1997), pp. 501–518.
2. R. S. Poethig, *Genetics* **119**, 959 (1988); M. M. S. Evans, H. J. Passas, R. S. Poethig, *Development* **120**, 1971 (1994); A. Telfer and R. S. Poethig, *Development* **125**, 1889 (1998); A. J. Ebens, H. Garren, B. N. R. Cheyette, S. L. Zipursky, *Cell* **74**, 15 (1993).
3. J. C. Dunlap, *Cell* **96**, 271 (1999).
4. Z. Liu, thesis, Harvard University (1990).
5. V. Ambros, *Cell* **57**, 49 (1989).
6. *lin-42* was mapped relative to the Tc1-induced RFLPs *nP48*, *veP1*, and *veP2* on the left arm of LG II as in B. D. Williams, B. Schrank, C. Huynh, R. Shownkeen, R. H. Waterston, *Genetics* **131**, 609 (1992). *veP1* and *veP2* were identified as Tc1-hybridizing Hind III RFLPs linked to and at left of *sup-9* (I. de la Cruz and R. Horvitz, personal communication). We cloned *veP1* and *veP2* into pBluescript SK$^-$ (Stratagene) by standard methods (*34*). *veP1* resides on cosmid K01A2 and *veP2* on cosmid T19G10.
7. *lin-4(e912); mut-6(st702); vels13* progeny were screened for Tc1-induced *lin-4* suppressors. *vels13* is an integrated array containing a *col-19::gfp* fusion (*8*), which is expressed adult-specifically in wild-type animals, and because its expression depends on hypodermal terminal differentiation, it is not expressed in *lin-4* mutants. We isolated 34 mutants with restored *col-19::gfp* expression from roughly 10^6 animals screened. Two putative *lin-42* mutations were outcrossed to wild-type males, yielding *lin-42(ve27)* and *ve32*. Several independent strains of *ve27* and *ve32* were outcrossed seven times, and a polymorphic 6.2-kb Eco RI restriction fragment that contained the transposon Tc1 and cosegregated with the *lin-42* mutant phenotype was identified and cloned. When sequences flanking the Tc1 insertion site in the 6.2-kb fragment were used in Southern blot analysis, they detected a polymorphism in genomic DNA from *ve27* and *ve32*, but not from wild-type (N2) animals, the parental strain, or several *lin-42* mutants induced by other means.
8. J. E. Abrahante, E. A. Miller, A. E. Rougvie, *Genetics* **149**, 1335 (1998).
9. The *C. elegans* Sequencing Consortium, *Science* **282**, 2012 (1998). Transformation was performed as described [C. C. Mello, J. M. Kramer, D. Stinchcomb, V. Ambros, *EMBO J.* **10**, 3959 (1991)]. Rescue was scored by the presence of lateral alae—cuticular ridges that are synthesized by adult seam cells. Because the precocious alae phenotype of *lin-42* mutants is sensitive to growth conditions (*8*), animals were hatched in the presence of food and grown at 20°C. At the concentrations injected (~100 ng/μl), we did not observe an overexpression phenotype. Multiple transgenic lines were examined for each construct.
10. A cDNA pool was prepared with an oligo$(dT)_{20}$ primer as described (*34*), and *lin-42* cDNA was amplified with primers from exons 2 and 5. An aliquot was reamplified with the exon 2 primer and a nested exon 5 primer. The DNA sequence of the product matched the GeneFinder prediction. Additional analyses confirmed the exon 1–2 splice pattern and revealed the trans-spliced leader SL1 at the 5′ end and no alternatively spliced products.
11. J. R. Nambu, J. O. Lewis, K. A. Wharton, S. T. Crews, *Cell* **67**, 1157 (1991); E. C. Hoffman *et al.*, *Science* **252**, 954 (1991).
12. S. T. Crews, J. B. Thomas, C. S. Goodman, *Cell* **52**, 143 (1988).
13. L. Saez and M. W. Young, *Neuron* **17**, 911 (1996).
14. B. Rost and C. Saunder, *J. Mol. Biol.* **232**, 584 (1993); *Proteins* **19**, 55 (1994).
15. P. E. Hardin, J. C. Hall, M. Rosbash, *Nature* **343**, 536 (1990).
16. I. L. Johnstone and J. D. Barry, *EMBO J.* **15**, 3633 (1996).
17. Developmentally staged cDNA pools (*16*) were PCR-amplified with primers specific for *lin-42*, *tim-1*, or *ama-1*. The primer sets were chosen to span an intron-exon boundary to distinguish cDNA- and genomic DNA–derived products. *ama-1* and *lin-42* reactions were incubated at 94°C for 1 min, followed by 27 cycles of 94°C for 30 s, 60°C for 30 s, and 72°C for 20 s with a PTC-100 thermocycler (MJ Research, Waltham, MA). For *tim-1* reactions, the extension time was 45 s. Reactions were terminated before any reagent became limiting. Dilutions of input cDNA and variation of amplification cycle numbers both indicated that the reactions were linear under these conditions. The amplified products were analyzed by Southern (DNA) blot using an end-labeled internal oligonucleotide as a probe (*34*). The blots were analyzed with a PhosphoImager and Image Quant software (Molecular Dynamics). The relative abundance of test cDNA (*lin-42* or *tim-1*) is expressed as the ratio of the test signal to that of *ama-1*. The amplifications and Southern blots were repeated three or four times for each gene. In each experiment, the time point with the highest value was set equal to one, and the remaining samples were expressed as a fraction thereof. The numbers for each time point were then averaged for each gene, and the ratios of *lin-42* and *tim-1* signals relative to *ama-1* were graphed (Fig. 3). The data do not measure the absolute levels of *lin-42* or *tim-1*. Complementary DNA pools for animals reared at 20°C were made as described (*16*).
18. C. G. Larminie and I. L. Johnstone, *DNA Cell Biol.* **15**, 75 (1996).
19. M. Jeon, H. F. Gardner, E. A. Miller, J. Deshler, A. E. Rougvie, data not shown.
20. A. Sehgal *et al.*, *Science* **270**, 808 (1995).
21. M. J. Zylka *et al.*, *Neuron* **21**, 1115 (1998).
22. A. M. Sangoram *et al.*, *Neuron* **21**, 1101 (1998).
23. N. Gekakis *et al.*, *Science* **270**, 811 (1995).
24. L. B. Vosshall, J. L. Price, A. Sehgal, L. Saez, M. W. Young, *Science* **263**, 1606 (1994).
25. T. K. Darlington *et al.*, *Science* **280**, 1599 (1998).
26. pMJ11 contains genomic DNA from the 5.5 kb upstream of the *lin-42* ATG to the last codon before the stop cloned in frame upstream of *gfp* in pPD95.75 (A. Fire, S. Xu, J. Ahnn, G. Seydoux, personal communication). In pMJ13, the *unc-54* 3′ UTR of pMJ11 was replaced with 1.3 kb of genomic DNA after the *lin-42* stop codon (Fig. 1). Transformation was into *lin-42(mg152)* (*9*). Both constructs rescue the *lin-42* mutant phenotype and give similar patterns of GFP expression. One array containing pMJ11 was integrated to yield *vels26*. LIN-42::GFP is also detected in vulval cells, pharyngeal cells, a few head neurons, and occasionally at low levels in the intestine.
27. J. C. Bettinger, K. Lee, A. E. Rougvie, *Development* **122**, 2517 (1996).
28. G. Ruvkun and J. Giusto, *Nature* **338**, 313 (1989).
29. E. G. Moss, R. C. Lee, V. Ambros, *Cell* **88**, 637 (1997).
30. R. C. Lee, R. L. Feinbaum, V. Ambros, *Cell* **75**, 843 (1993); B. Wightman, I. Ha, G. Ruvkun, *Cell* **75**, 855 (1993).
31. M. Jeon and A. Rougvie, unpublished results.
32. M. C. Lindebro, L. Poellinger, M. L. Whitelaw, *EMBO J.* **14**, 3528 (1995).
33. K. Iwasaki, D. W. C. Liu, J. H. Thomas, *Proc. Natl. Acad. Sci. U.S.A.* **92**, 10317 (1995).
34. F. M. Ausubel *et al.*, Eds. (Wiley, New York, 1994).
35. Single-letter abbreviations for the amino acid residues are as follows: A, Ala; C, Cys; D, Asp; E, Glu; F, Phe; G, Gly; H, His; I, Ile; K, Lys; L, Leu; M, Met; N, Asn; P, Pro; Q, Gln; R, Arg; S, Ser; T, Thr; V, Val; W, Trp; and Y, Tyr.

36. D. P. King *et al.*, *Cell* **89**, 641 (1997).
37. We thank I. Johnstone for providing the 25°C cDNA pools; I. de la Cruz for sharing LGII information; the Ruvkun lab for the *mg152* allele; the Ambros lab for the *ma172* allele; M. Simmons and the Twin Cities Worm Community for advice and discussions; J. Simon, M. Peifer, and J. Shaw for manuscript critiques; Y. Kohara for the *tim-1* cDNAs; and M. Sanders and D. Gartner for imaging help. Supported by NIH Predoctoral Training Grant HD007480 to H.F.G. and NIH grant GM50227 to A.E.R.

29 April 1999; accepted 27 September 1999

An Adenosine Deaminase that Generates Inosine at the Wobble Position of tRNAs

André P. Gerber and Walter Keller*

Several transfer RNAs (tRNAs) contain inosine (I) at the first position of their anticodon (position 34); this modification is thought to enlarge the codon recognition capacity during protein synthesis. The tRNA-specific adenosine deaminase of *Saccharomyces cerevisiae* that forms I_{34} in tRNAs is described. The heterodimeric enzyme consists of two sequence-related subunits (Tad2p/ADAT2 and Tad3p/ADAT3), both of which contain cytidine deaminase (CDA) motifs. Each subunit is encoded by an essential gene (*TAD2* and *TAD3*), indicating that I_{34} is an indispensable base modification in elongating tRNAs. These results provide an evolutionary link between the CDA superfamily and RNA-dependent adenosine deaminases (ADARs/ADATs).

It has been known for 35 years that inosine occurs at the wobble position of tRNA anticodons (*1*, *2*), and it was postulated that these tRNAs can translate three codons ending in U, C, or A (*3*). This important modification occurs in eight cytoplasmic tRNAs in higher eukaryotes (seven in yeast) and in $tRNA_2^{Arg}$ from prokaryotes and plant chloroplasts (*4*). I_{34} is thereby formed by hydrolytic deamination of a genomically encoded adenosine (A), and the enzymatic activity for this RNA editing reaction has been partially purified from yeast (*5*, *6*). A family of mammalian adenosine deaminases (ADARs) that convert A to I in double-stranded RNA (dsRNA) and edit diverse cellular mRNA precursors (pre- mRNAs) has been identified (*7*), but none of these enzymes forms I in tRNA. Recently, a yeast and human protein that acts on tRNA has been cloned by sequence

Department of Cell Biology, Biozentrum, University of Basel, 4056 Basel, Switzerland.

*To whom correspondence should be addressed. E-mail: walter.keller@unibas.ch

http://www.jstor.org

LINKED CITATIONS

- Page 1 of 2 -

You have printed the following article:

Similarity of the C. elegans Developmental Timing Protein LIN-42 to Circadian Rhythm Proteins

Mili Jeon; Heather F. Gardner; Eric A. Miller; Jodie Deshler; Ann E. Rougvie

Science, New Series, Vol. 286, No. 5442. (Nov. 5, 1999), pp. 1141-1146.

Stable URL:

http://links.jstor.org/sici?sici=0036-8075%2819991105%293%3A286%3A5442%3C1141%3ASOTCED%3E2.0.CO%3B2-3

This article references the following linked citations:

References and Notes

[9] **Genome Sequence of the Nematode C. elegans: A Platform for Investigating Biology**

The C. elegans Sequencing Consortium

Science, New Series, Vol. 282, No. 5396. (Dec. 11, 1998), pp. 2012-2018.

Stable URL:

http://links.jstor.org/sici?sici=0036-8075%2819981211%293%3A282%3A5396%3C2012%3AGSOTNC%3E2.0.CO%3B2-M

[11] **Cloning of a Factor Required for Activity of the Ah (Dioxin) Receptor**

Emily C. Hoffman; Herminio Reyes; Fong-Fong Chu; Fred Sander; Linda H. Conley; Barbara A. Brooks; Oliver Hankinson

Science, New Series, Vol. 252, No. 5008. (May 17, 1991), pp. 954-958.

Stable URL:

http://links.jstor.org/sici?sici=0036-8075%2819910517%293%3A252%3A5008%3C954%3ACOAFRF%3E2.0.CO%3B2-%23

[20] **Rhythmic Expression of timeless: A Basis for Promoting Circadian Cycles in period Gene Autoregulation**

Amita Sehgal; Adrian Rothenfluh-Hilfiker; Melissa Hunter-Ensor; Yifeng Chen; Michael P. Myers; Michael W. Young

Science, New Series, Vol. 270, No. 5237. (Nov. 3, 1995), pp. 808-810.

Stable URL:

http://links.jstor.org/sici?sici=0036-8075%2819951103%293%3A270%3A5237%3C808%3AREOTAB%3E2.0.CO%3B2-5

NOTE: *The reference numbering from the original has been maintained in this citation list.*

http://www.jstor.org

LINKED CITATIONS

[23] **Isolation of timeless by PER Protein Interaction: Defective Interaction Between timeless Protein and Long-Period Mutant PER^L**

Nicholas Gekakis; Lino Saez; Anne-Marie Delahaye-Brown; Michael P. Myers; Amita Sehgal; Michael W. Young; Charles J. Weitz

Science, New Series, Vol. 270, No. 5237. (Nov. 3, 1995), pp. 811-815.

Stable URL:

http://links.jstor.org/sici?sici=0036-8075%2819951103%293%3A270%3A5237%3C811%3AIOTBPP%3E2.0.CO%3B2-H

[24] **Block in Nuclear Localization of period Protein by a Second Clock Mutation, timeless**

Leslie B. Vosshall; Jeffrey L. Price; Amita Sehgal; Lino Saez; Michael W. Young

Science, New Series, Vol. 263, No. 5153. (Mar. 18, 1994), pp. 1606-1609.

Stable URL:

http://links.jstor.org/sici?sici=0036-8075%2819940318%293%3A263%3A5153%3C1606%3ABINLOP%3E2.0.CO%3B2-O

[25] **Closing the Circadian Loop: CLOCK-Induced Transcription of Its Own Inhibitors per and tim**

Thomas K. Darlington; Karen Wager-Smith; M. Fernanda Ceriani; David Staknis; Nicholas Gekakis; Thomas D. L. Steeves; Charles J. Weitz; Joseph S. Takahashi; Steve A. Kay

Science, New Series, Vol. 280, No. 5369. (Jun. 5, 1998), pp. 1599-1603.

Stable URL:

http://links.jstor.org/sici?sici=0036-8075%2819980605%293%3A280%3A5369%3C1599%3ACTCLCT%3E2.0.CO%3B2-H

[33] **Genes that Control a Temperature-Compensated Ultradian Clock in Caenorhabditis elegans**

Kouichi Iwasaki; Dennis W. C. Liu; James H. Thomas

Proceedings of the National Academy of Sciences of the United States of America, Vol. 92, No. 22. (Oct. 24, 1995), pp. 10317-10321.

Stable URL:

http://links.jstor.org/sici?sici=0027-8424%2819951024%2992%3A22%3C10317%3AGTCATU%3E2.0.CO%3B2-V

NOTE: *The reference numbering from the original has been maintained in this citation list.*